Science of the Total Environment 409 (2011) 968–978

Contents lists available at ScienceDirect

Science of the Total Environment

journal homepage: www.elsevier.com/locate/scitotenv

Biogeochemical factors influencing net mercury methylation in contaminated freshwater sediments from the St. Lawrence River in Cornwall, Ontario, Canada

Mary-Luyza Avramescu [a], Emmanuel Yumvihoze [a], Holger Hintelmann [b], Jeff Ridal [c], Danielle Fortin [d,*], David R.S. Lean [a]

[a] Biology Department, University of Ottawa, 30 Marie Curie, Ottawa, ON, Canada, K1N 6N5
[b] Chemistry Department, Trent University, 1600 West Bank Drive, Peterborough, ON, Canada K9J 7B8
[c] St. Lawrence River Institute of Environmental Sciences, 2 Belmont Street, Cornwall, ON, Canada, K6H 4Z1
[d] Earth Science Department, University of Ottawa, 140 Louis Pasteur, Ottawa, ON, Canada, K1N 6N5

ARTICLE INFO

Article history:
Received 26 August 2010
Received in revised form 14 November 2010
Accepted 16 November 2010
Available online 21 December 2010

Keywords:
Methylmercury
Methylation
Demethylation
SRB
MPA
FeRP
Sediments

ABSTRACT

The activity of various anaerobic microbes, including sulfate reducers (SRB), iron reducers (FeRP) and methanogens (MPA) has been linked to mercury methylation in aquatic systems, although the relative importance of each microbial group in the overall process is poorly understood in natural sediments. The present study focused on the biogeochemical factors (i.e. the relative importance of various groups of anaerobic microbes (FeRP, SRB, and MPA) that affect net monomethylmercury (MMHg) formation in contaminated sediments of the St. Lawrence River (SRL) near Cornwall (Zone 1), Ontario, Canada. Methylation and demethylation potentials were measured separately by using isotope-enriched mercury species ($^{200}Hg^{2+}$ and $MM^{199}Hg^{+}$) in sediment microcosms treated with specific microbial inhibitors. Sediments were sampled and incubated in the dark at room temperature in an anaerobic chamber for 96 h. The potential methylation rate constants (K_m) and demethylation rates (K_d) were found to differ significantly between microcosms. The MPA-inhibited microcosm had the highest potential methylation rate constant (0.016 d^{-1}), whereas the two SRB-inhibited microcosms had comparable potential methylation rate constants (0.003 d^{-1} and 0.002 d^{-1}, respectively). The inhibition of methanogens stimulated net methylation by inhibiting demethylationand by stimulating methylation along with SRB activity. The inhibition of both methanogens and SRB was found to enhance the iron reduction rates but did not completely stop MMHg production. The strong positive correlation between K_m and Sulfate Reduction Rates (SRR) and between K_d and Methane Production Rates (MPR) supports the involvement of SRB in Hg methylation and MPA in MMHg demethylation in the sediments. In contrast, the strong negative correlation between K_d and Iron Reduction Rates (FeRR) shows that the increase in FeRR corresponds to a decrease in demethylation, indicating that iron reduction may influence net methylation in the SLR sediments by decreasing demethylation rather than favouring methylation.

1. Introduction

Mercury methylation in aquatic systems has been linked to the activity of various anaerobic microbes, including sulfate reducers, iron reducers and methanogens (i.e., Wood et al., 1968; Compeau and Bartha, 1985; Flemming et al., 2006; Barkay et al., 2003; Benoit et al., 2003). Despite a large body of research with pure microbial cultures, little is known about the relative importance of each microbial group in the overall process of mercury methylation in natural sediments.

Although many studies have confirmed the natural conversion of inorganic mercury to methyl mercury, the mechanism itself remains elusive. Previous studies have shown that bacteria play a role in mercury methylation, especially sulphate-reducing bacteria (SRB) (Compeau and Bartha, 1985; Gilmour and Henry, 1991; Merritt and Amirbahman, 2009), however not all SRB are capable of mercury methylation (King et al., 2000; Ullrich et al., 2001). Other micro-organisms, including methanogens (MPB) and iron-reducing bacteria (FeRB) may also be important (Wood et al., 1968; Pak and Bartha, 1998; Flemming et al., 2006; Kerin et al., 2006). This ability to convert mercury to methyl mercury may well have been a protective mechanism during the early evolution of those microbes some three billion years ago (Clarkson, 1998). It is also becoming clear that we must also distinguish biotic (microbial) from abiotic (chemical) processes.

The environmental concentrations of MeHg reflect net methylation rather than actual rates of MeHg synthesis, leading to a near

Abbreviations: MMHg, methylmercury; ^{200}Hg, mercury enriched with ^{200}Hg; $MM^{199}Hg$, methylmercury enriched with ^{199}Hg; $MM^{200}Hg$, methylmercury enriched with ^{200}Hg; MPA, methanogens; FeRP, iron-reducing prokaryotes; SRB, sulfate-reducing bacteria; SRR, sulfate reduction rates; FeRR, iron reduction rates; MPR, methane production rates.

* Corresponding author. Tel.: +1 613 562 5800x6423; fax: +1 613 562 5192.
E-mail address: dfortin@uottawa.ca (D. Fortin).

0048-9697/$ – see front matter © 2010 Elsevier B.V. All rights reserved.
doi:10.1016/j.scitotenv.2010.11.016

constant level of MeHg which rarely exceeds 1 to 1.5% of THg in sediments. Few studies (i.e., Hintelmann et al., 2000; Martin-Doimeadios et al., 2004; Heyes et al., 2006; Drott et al., 2008a,b) provide information about both simultaneous methylation and demethylation processes, nor do we know which organisms, if any, are responsible. Previous investigations have concluded that both processes are very rapid, and the net formation of methyl mercury may be near zero even though reaction rates may be high in both directions (Eckley et al., 2005; Eckley and Hintelmann, 2006; Hintelmann et al., 2000; Hintelmann and Ogrinc, 2003). A recent review (Merritt and Amirbahman, 2009) exploring the mechanisms hypothesised to influence aqueous phase and sediment solid phase MMHg concentrations and depth-specific inorganic Hg (II) methylation rates within estuarine and coastal marine environments recognized that the processes responsible for MeHg production and consumption overlap spatially and/or kinetically in sedimentary environments, and likely dictate the extent to which MMHg accumulates. Therefore, they concluded that kinetic models were required to understand MeHg production and consumption in these environments.

The present study focussed on the contaminated sediments of the St. Lawrence River (SLR) near Cornwall, Ontario, Canada. The area between Moses-Saunders Dam and the Beauharmois Dam in Quebec has been designated a Great Lakes' "Area of Concern" (AOC) by the International Joint Commission (IJC) in 1985 (Richman and Dreier, 2001; Ridal et al., 2009). The river's ecosystem has been affected by chemical pollution (heavy metals, such as Hg, Zn, Pb, Cu, etc. and organic compounds), which has resulted in habitat degradation in the area (Quemarais et al., 1998). The main source of Hg in the river sediments originates from historical point source discharges from local industries including textile, pulp and paper, and mercury cell chlor-alkali (Richman and Dreier, 2001; Delongchamp et al., 2009). Although other sources, such as tributaries discharging agricultural and wetland runoff, diffuse sources from Lake Ontario and long-range atmospheric transport and deposition, may also be important (Ridal et al., 2009).

We investigated factors potentially controlling net monomethylmercury (MMHg) formation in surficial sediments of the St. Lawrence AOC, specifically the role played by methanogens (MPA), iron-reducing prokaryotes (FeRP) and sulfate-reducing bacteria (SRB) in the St. Lawrence River sediments. River sediments were incubated with isotope-enriched mercury compounds and specific microbial inhibitors. The MMHg formation and degradation rates were calculated and correlated with activity rates of anaerobic microbes (SRB, MPA, and FeRP) and geochemical parameters. The main objectives of this study were: (a) to determine the rates of abiotic and biotic methylmercury formation and demethylation, (b) to assess the relative contribution of the different groups of anaerobic microbes (SRB, MPA, and FeRP) to methylmercury formation and demethylation in freshwater sediments, and (c) to assess the relationship between the geochemical characteristics of the porewaters (i.e., pH, Eh, sulfide, sulfate, ferrous and ferric iron) and methylmercury formation and demethylation in St. Lawrence River sediments. We originally hypothesized that abiotic methylation would represent an important pathway for Hg methylation (i.e., Baldi et al., 1995; Falter, 1999; Celo et al., 2006) and that the inhibition of sulfate reducers would favor the growth of iron reducers and the formation of MeHg (i.e., Flemming et al., 2006; Kerin et al., 2006).

2. Materials and methods

2.1. Site description

Hg concentrations in the sediments of three main depositional areas (zones 1, 2 and 3, as in Delongchamp et al., 2009) in the St-Lawrence River near Cornwall, Ontario, Canada, exceed the Canadian Sediment Quality Guidelines for the protection of aquatic organisms (Interim sediment quality guidelines: 0.170 mg/kg; Probable Effect Level: 0.486 mg/kg) (Canadian Council of Ministers of the Environment, 2005).

There is a high rate of methane production in zone 1 (Poissant et al., 2007; Razavi, 2008) and sedimentation rates range from 0.18 to 0.58 g cm^{-2} $year^{-1}$ along the Cornwall waterfront (Delongchamp et al., 2009). Despite the closure of the main industrial sources of Hg to the area, the contaminated sediments remain to be a potential source of MMHg to the riparian ecosystem. (Delongchamp et al., 2009). A natural remediation strategy was adopted, and the sediments were left in place where they were subject to burial by sediments with a low Hg content. However, investigation of the recently deposited surficial sediments indicated that even though they are less contaminated in THg, they are more contaminated in MMHg than deeper sediments, with almost 6% MMHg in the top 1 cm in Zone 1 (Delongchamp et al., 2009).

Zone 1, the subject of this study, shows high spatial sediment heterogeneity characterized by large deposits of decaying bark and wood chips overlaid by fine-grained sediments with high concentrations of Hg (Biberhofer and Rukavina, 2002). In some places, the sediments are a composite of brown-black clay and mud with wood fibers and oil patches resulting from the historical industrial contamination of the site (Delongchamp et al., 2009) and the microbial decomposition of wood fibers from the pulp and paper mill, which has resulted in a high gas production (72% of the muddy deposit in this zone contains a high gas content) (Poissant et al., 2007).

2.2. Sample collection

Surface water and sediment samples were collected from the Zone 1 of the St. Lawrence River in Cornwall in the summer of 2007. Surface sediments from Zone 1 were sampled using plastic tubes (10 cm in diameter and 1 m in length) that were sealed on the top to prevent oxygen from contacting the samples and they were kept cold during handling. The cores were taken at the same location (within a 1 m × 1 m area), sliced (0–5 cm) in the field and transferred into in 3–5 L acid washed high density polyethylene (HDPE) bottles under a nitrogen atmosphere in order to prevent contact with oxygen, and were kept on ice during their transport to the laboratory.

In the laboratory, the pooled sediments (i.e., the 0–5 cm layers of different cores) were homogenized and sediment sub-samples were transferred into sterile 500 mL brown HDPE bottles under a nitrogen atmosphere and subsequently used for the microcosm incubations with isotope-enriched Hg tracers and microbial inhibitors. The time lag between sampling and the start of the incubation was 48 h, during which time the samples were stored in the dark at 4 °C. Sub-samples were transferred anaerobically to centrifuge tubes for geochemical, microbial, and total Hg (THg) and MMHg analyses.

Surface water from above the sediment–water interface was sampled and collected in acid washed HDPE bottles. *In situ* pH and Eh measurements were performed for the July samples using a portable pH meter (VWR, Model SP21) and pH and ORP-probes. Water conductivity and dissolved oxygen were also measured on site (VWR, Model SP21and YSI, Model 54). Samples were kept refrigerated (4 °C) and analyzed for sulfate, nitrate, and total phosphorus within three weeks of sampling.

2.3. Hg methylation–MMHg demethylation experiment set-up

Environmental concentrations of MMHg reflect net production, which is the result of two simultaneous reactions: Hg methylation and MMHg degradation. Our experiments were designed to measure gross rates of MMHg formation and demethylation and to assess the relative contribution of different types of anaerobic microbes involved in MMHg formation and demethylation, by combining the isotope-enriched

multilabeling technique (Hintelmann et al., 1995; Hintelmann and Evans, 1997) to determine mercury species transformation rates (i.e., Hg methylation and MMHg demethylation rates) using stable isotope-enriched mercury species (Hintelmann et al., 2000; Hintelmann and Ogrinc, 2003).

In order to assess the relative contribution of different types of anaerobic microbes in methylmercury formation and demethylation, specific inhibitors of SRB (sodium molybdate ($NaMoO_4$)) (Chen et al., 1996; Pak and Bartha, 1998) and MPA (sodium 2-bromoethane sulfonate (BES)) (Balch and Wolfe, 1979; Compeau and Bartha, 1985) were added to the microcosms prior to the addition of isotope-enriched Hg tracers. There is no known inhibitor for iron-reducing prokaryotes (FeRP).

The experimental set-up and the description of all microcosms are presented in Table 1. Microcosms containing the St. Lawrence River sediment slurry (0–5 cm) were inoculated in triplicates with stable isotope-enriched mercury (^{200}Hg and $Me^{199}Hg$), treated with specific microbial inhibitors ($NaMoO_4$ and BES) and incubated in dark HDPE bottles (cca. 500 g of homogenized sediments per replicate) at room temperature in an anaerobic chamber for 96 h. Details of the Hg spike and microbial inhibitor additions are given in Table 2. Sub-samples were removed at various time intervals (0, 24, 46, 72, and 96 h) to measure the amount of $Me^{200}Hg$ produced and the amount of $Me^{199}Hg$ removed (i.e., Martin-Doimeadios et al., 2004). Temperature, pH, Eh, water and organic matter content (LOI), along with sulfate reduction rates (SRR) and methane production rates (MPR) were determined on separate sub-samples. The porewater was extracted immediately after sampling: subsequent analyses of soluble Fe(II) and sulfides were conducted within minutes after the extraction in the anaerobic chamber and sub-samples for Hg isotopic analyses were acidified and kept frozen until analysis. Sulfate reduction rates and methane production rates were determined in parallel in triplicates for all of the microcosms, as described below. Isotope-enriched ^{200}HgO, $Me^{199}HgCl$, and $Me^{201}HgCl$ used for this study were kindly provided by Dr. Hintelmann (Trent University). $Me^{199}HgCl$ and $Me^{201}HgCl$ were prepared at Trent University from enriched 199HgO and ^{201}HgO, respectively. Stock solutions of 706 μg/mL of $Me^{199}HgCl$ in 2-propanol and 911 μg/mL $^{200}Hg^{2+}$ in 10% nitric acid were diluted appropriately on the day of spiking, using anoxic overlaying water from the sampling site. The added tracers were equilibrated in overlaying water for two hours before being added to the incubation bottles in order to achieve the same speciation as the ambient Hg(II) (Hintelmann et al., 2000; Hammerschmidt et al., 2004; Drott et al., 2008b). A minimum amount of isotope-enriched spike is required for the species transformation assay to ensure that the excess of isotope-enriched MMHg is detectable against the natural MMHg background. At least 1% of the total MMHg should be in isotope-enriched form, which was usually achieved during the experiments in this study. The spike additions increased the concentrations of total Hg by approximately 10% and doubled that of methylmercury, when compared to the background ambient MMHg concentrations (Table 3). The ambient background concentrations of the St. Lawrence sediments used for the incubation experiments along with the concentrations after the isotope addition are shown in Table 2.

Naturally occurring SRB activity was inhibited by treating the sediment slurries with sodium molybdate ($NaMoO_4$) (Chen et al., 1996; Pak and Bartha, 1998) to a final concentration of approximately 1.8 mM. This treatment also prevented FeS formation. The precipitation of FeS may lead to an underestimation of iron reduction rates (FeRR) if rates are determined from the increase of dissolved Fe(II) concentrations. The efficiency of $NaMoO_4$ to inhibit sulfate reduction was determined by comparison of the SRR in triplicate sub-samples (t = 0 h) from amended and not amended sediments. Naturally occurring methanogens were inhibited by treating the sediment slurries with sodium 2-bromoethane sulfonate (BES, $BrCH_2CH_2SO_3Na$) (Balch and Wolfe, 1979; Compeau and Bartha, 1985; Oremland and Capone, 1988) to a final concentration of approximately 30 μM. The efficiency of BES as an inhibitor was later tested by measuring the headspace methane concentrations during all three experiments.

Table 1
Microcosm set-up and description. The sampling times (t) were 0, 24, 46, 72 and 96 h.

Microcosm ID	Microcosm description (n = 3 replicate bottles)	Mercury spikes/inhibitors added		
		$^{200}Hg^{2+}$ and $MM^{199}Hg^{+}$ spikes	SRB inhibitor ($NaMoO_4$)	MPA inhibitor (BES)[a]
N1	Natural (unspiked control)	No	No	No
T1	Hg spiked control	Yes[b]	No	No
T2	SRB inhibited	Yes[b]	Yes[c]	No
T3	MPA inhibited	Yes[b]	no	Yes[d]
T4	SRB and MPA inhibited	Yes[b]	Yes[c]	Yes4
A1	Hg spiked Abiotic control (Autoclaved sediments at 105 °C three times for 45 min)	Yes[b]	No	No

[a] BES: sodium 2-bromoethane sulfonate.
[b] Isotope-enriched Hg solutions were added to give a final concentration of approximately 77.7 ng/g $^{200}Hg^{2+}$ (1.1 mL of 10.743 μg/mL $^{200}Hg^{2+}$) and approximately 4.7 ng/g $Me^{199}Hg^{+}$ (1.1 mL of 647.2 ng/mL $Me^{199}Hg$) in the sediment slurry.
[c] 1.4 mM final concentration of molybdate in the sediments (2.5 mL of 250 mM NaMoO4).
[d] 28 mM final concentration of BES in the sediments (6.3 mL of cca 2 M BES).

2.4. Sample analysis

Two categories of samples were analyzed: (a) water and sediment samples preserved in the field and (b) sediments and porewater samples taken from the microcosm incubation experiments designed to determine the potential Hg methylation and MMHg demethylation rates. Analyses performed on the samples preserved in the field included sediment THg, MMHg, water and organic carbon content (as loss on ignition (LOI)), as well as porewater sulfate, sulfide and Fe(II). The analytical measurements associated with the samples originating from the microcosm incubations included sediment THg and MMHg isotopic analyses, sulfate reduction rate, iron reduction rates , methane production rate, water and organic carbon content (as LOI), pH and Eh, as well as porewater sulfide and ferrous iron (Fe(II)). The porewater samples from the incubation experiment were extracted by centrifugation (Beckman J2-MC centrifuge) at 5000 rpm for 20 min at 4 °C, immediately transferred to a clean syringe, and filtered through 0.22 μm syringe filters (Millex GP 0.22 μm, Millipore cat. no. SLGP033RS). All porewater analyses (i.e. Fe(II) and sulfides) were performed the same day that the waters were extracted from the incubated sediments.

2.4.1. Mercury analysis

Total Hg and MMHg concentrations were measured in wet sediment samples and normalized to dry weight based on the water content of the samples in order to avoid losses and changes in Hg speciation that would be encountered during the drying process.

The total Hg isotopic compositions of the sediments from the incubation experiments were determined at Trent University (Ontario, Canada), after acid digestion by continuous-flow cold vapor generation and detection by ICP-MS, as described in Hintelmann and Ogrinc (2003). Methylmercury isotope analysis of the sediments from the microcosm incubation experiments was conducted using the Thiosulfate method (TSE) (Avramescu et al., 2010) and the distillation–aqueous–ethylation method (Hintelmann and Ogrinc, 2003), as described in Avramescu et al. (2010). To correct for procedural recoveries, each sample was spiked with $Me^{201}Hg$ prior to digestion or distillation, respectively. The Hg isotopes measured were ^{202}Hg (to calculate ambient MMHg concentrations), ^{200}Hg (methylation spike), ^{199}Hg (demethylation spike) and ^{201}Hg (internal standard). Peak areas were used to calculate the concentrations of individual isotopes accounting for procedural blanks, as described in Hintelmann and Ogrinc (2003). The sample

Table 2
Sediment ambient background concentrations and percentage increases due to isotope-enriched Hg ($^{200}Hg^{2+}$ and $MM^{199}Hg$) additions in the St. Lawrence River incubation experiment. Standard errors are given (±SE) where n ≥ 2.

Parameter	N1	T1	T2	T3	T4	A1
Organic content (±SE), (%) n = 3	7.7 (0.1)	7.9 (0.1)	7.9 (0.1)	9.2 (0.1)	9.0 (0.1)	8.2 (0.1)
Water content (±SE), (%) n = 3	73.3 (2.6)	70.4 (0.1)	70.8 (0.1)	70.9 (0.0)	70.9 (0.1)	72.4 (1.2)
Ambient THg, ng/g, n = 1	1079	1593	866	1790	1790	982
Ambient MMHg (±SD), ng/g, n = 2	2.9 (0.0)	2.5 (0.1)	2.6 (0.1)	3.3 (0.8)	2.9 (0.2)	1.8 (0.2)
THg (±SD) after spike additions, ng/g, n = 2	751 (280)	820 (140)	1106	907 (11)	1212 (70)	2018 (1538)
MMHg (±SD) after $Me^{199}Hg$ addition, ng/g, n = 2	2.6 (0.0)	7.0 (0.01)	8.2 (0.7)	8.9 (0.5)	8.4 (1.1)	6.2 (0.3)
^{200}Hg addition (±SD)	n.a.[a]	61.5 (0.3)	72.2 (18.6)	66.2 (0.4)	76.7 (8.6)	67.7 (6.0)
$Me^{199}Hg$ addition (±SD)	n.a.	4.1 (0.1)	5.1 (0.5)	5.4 (0.3)	5.2 (0.5)	4.3 (0.2)
Factor increase[b] in THg due to ^{200}Hg and $Me^{199}Hg$	n.a.	1×	1.1×	1×	1×	1.1×
Factor increase in MMHg due to $Me^{199}Hg$	n.a.	2.8×	3.2×	2.7×	2.9×	3.5×
% MMHg initial	n.a.	0.2%	0.3%	0.2%	0.2%	0.2%
% MMHg after spiking	n.a.	0.4%	0.9%	0.5%	0.5%	0.6%
increase in % MMHg	n.a.	0.3%	0.6%	0.3%	0.3%	0.4%

[a] not available.
[b] Due to the high variability of the ambient THg in the SLR sediments (751 to 2018 ng/g dw), the increase in THg due to Hg spike addition was calculated considering: $[THg]_{(after\ spike\ addition)} = [THg]_{(before\ spike\ additions)} + [^{200}Hg] + [^{199}Hg]$.

relative standard errors (RSE; standard error/mean) varied between 1 and 6%. MMHg reference materials (BCR 580, IAEA 405) were analyzed (n = 6–8) with both methods as part of the QA/QC protocol. Recoveries of 94 to 109% were obtained for both certified reference materials (CRM) with both procedures (i.e., BCR 580: 97.1%, n = 6, RSD = 0.43 and IAEA 405: 98.2%, n = 8, RSD = 2.69). The accuracy of the CRM measurements, calculated as the percent error of the mean of the measurements, was 0.26% for BCR 580 and 1.8% for IAEA 405. The MMHg concentration in the reagent blanks was below the detection limit of 1 pg of MMHg (as Hg) for the TSE and distillation procedure.

2.4.2. Geochemical analyses

The water content of the sediment samples was determined by drying the sediments for 24 h at 105 °C, and the organic carbon content was estimated by loss on ignition (LOI) by heating the samples at 400 °C for 8 h. Total sulfate concentrations in porewater samples were determined with the $BaSO_4$ turbidimetric method (Rodier, 1997), whereas sulfides were analyzed with the Cline's colorimetric method (range: 0–2.5 μM) (Cline, 1969). Ferrous iron concentrations in porewater were determined using the revised ferrozine method (Viollier et al., 2000), using a Cary 100 UV–Vis spectrophotometer (562 nm, MDL = 0–5.5 mg/L). Sulfide and iron analyses were performed within minutes after the porewaters were extracted in order to prevent oxidation. Nitrate and total phosphorus in overlaying water were measured with a Quick Chem Series 8000 Lachat Instrument using the Quick Chem Method 10-107-04-1-C (range 0.01 to 2.0 mgN/L as NO^{3-}; MDL as 0.002 mgN/L; potassium nitrate (Sigma Aldrich 204110-50G) standards) and Quick Chem Method 10-115-01-3-A (range 0.1 to 10 mgP/L; MDL as 0.007 mgP/L; potassium phosphate monobasic (EM Science B10203-34) standards) respectively.

Table 3
Total percentage of mercury methylated and methylmercury demethylated from the spikes in the different systems (calculated by dividing the amount measured by the amount spiked ×100).

Microcosm	Ambient Hg[a]		Methylated inorganic spike[a]		Demethylated MMHg spike	
	46 h	96 h	46 h	96 h	46 h	96 h
N1	0.3	0.3	n/a	n/a	n/a	n/a
T1	0.4	0.4	9.4	9.7	14.3	40.4
T2	0.3	0.3	2.7	2.6	16.2	44.4
T3	0.4	0.5	10.5	11.3	8.1	6.8
T4	0.25	0.28	1.9	2.1	4.2	1.6
A1	0.1	0.2	0.4	0.4	−8.8	−10.4

[a] Percentage of the methylated Hg (%[MMHg]/[Hg^{2+}]) was calculated considering $Hg^{2+} = [THg] - [MMHg]$.

The metabolic activity of iron-reducing prokaryotes in sediments was determined by measuring the *in situ* iron reduction rates (Wendt-Potthoff et al., 2002). Iron reduction rates (nmol $Fe^{2+}/cm^3/d$) were determined in triplicate by linear regression of porewater Fe(II) concentrations overtime. Sulfate reduction rates (SRR) were determined in triplicate for all microcosms (t = 0 h) according to Jørgensen (1978), as described in Praharaj and Fortin (2004). As described in Meier et al. (2000), SRR (nmol $SO_4^{2-}/cm^3/d$) were calculated based on the S-35 radioactivity and taking into account the porosity values.

The metabolic activity of methanogenic archaea (MPA) was determined by measuring the *in situ* methane production rates (MPR), using the headspace method described in Koschorreck (2000). Immediately after adding the Hg spikes and inhibitors, 100 mL sediment slurry was transferred in an anaerobic chamber into 125 mL serum glass bottles and crimp-sealed. The gas in the headspace was extracted at the same time as the sediment sub-samples. After vigorous shaking for 5 min and 30 min of headspace equilibration, 10 mL gas samples from the headspace were transferred into 12 mL vacutainers and analyzed using GC-FID (SRI8610C, with an unheated splitless injector).

2.5. Potential methylation rate constant calculation

The rates of mercury methylation and demethylation of methylmercury in sediments were expressed in pmol/g/h of ^{200}Hg methylated and of $Me^{202}Hg$ demethylated, respectively. Pseudo-first order reaction kinetics were assumed to calculate potential methylation (K_m) and demethylation rate (K_d) constants following the procedure outlined in Hintelmann et al. (2000).

2.6. Statistical analyses

Simple linear regression was used to calculate FeRR for the different microcosms over a 46 h incubation period, and to determine relationships between the porewater characteristics and different MMHg isotope concentrations using the S-Plus 8.0 software for Windows. Analysis of variance (ANOVA) with multiple comparisons (Bonferroni, Schaefer, and Tukey methods) was also performed (Zar, 2006; Otto, 2007) to assess if the differences between the SRR, FeRR, and MPR were significant among microcosms. The XLfit software was also used to determine ambient K_m and K_d values by curve fitting the ambient MMHg data.

3. Results and discussion

3.1. Field data results

The physico-chemical characteristics of the overlying and sediment porewater at the St. Lawrence River (Zone 1) sampling site are

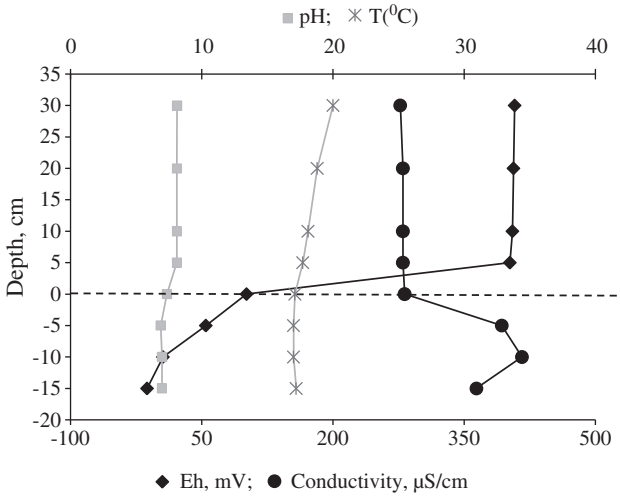

Fig. 1. Physico-chemical characteristics of the porewaters and overlying water at the St. Lawrence River site (Cornwall, On., summer 2007) as a function of depth: Eh (mv); conductivity (µs/cm); temperature (°C); and pH. The dotted line represents the sediment (S)–water (W) interface.

presented in Fig. 1. The river water (i.e., water above the sediment–water interface) is slightly alkaline (pH = 8.11) and moderately hard (conductivity = 279.3 ± 1.5 µS/cm, n = 4), with low levels of sulfate (25.6 ± 1.01 mg/L, n = 4) and nitrate (0.22 ± 0.04 mgN/L, n = 4), but higher levels of total phosphorous (38.6 ± 0.0 µgP/L, n = 2). The pH of the porewaters slightly decreased with sediment depth from 7.35 to 6.97 (0–15 cm), whereas there was a sharp redox boundary at the sediment–water interface. Porewaters (n = 4) contain low levels of sulfate (20.6 ± 4.5 µM), sulfide (1.5 ± 0.3 µM) and ferrous iron (14.5 ± 3.2 µM). The surface sediments (0–5 cm depth, n = 3 cores) have a density of 1.2 ± 0.01 g/cm^3 and a porosity of 0.83 ± 0.02 g/cm^3, and contain on average ~9.8 ± 0.4% of organic carbon (as LOI) with a moisture content of 69.7 ± 1.5%. Total mercury (THg) and methylmercury concentrations (n = 3) of the sediments varied between 1180 ± 373 ng/g and 0.9 ± 0.2 ng/g, respectively. All of our results were in agreement with previous geochemical studies of the St. Lawrence River (Canario et al., 2009; Delongchamp et al., 2009, 2010).

3.2. Hg methylation and MMHg demethylation

The porewater characteristics, along with the sulfate and iron reduction rates and methane production rates in the six systems tested (i.e., N1, T1, T2, T3, T4, and A1 as described in Table 1) are presented in Figs. 2 and 3. Geochemical analyses are presented as an average of three replicates (±SD), although only two replicates were analyzed for concentrations of individual mercury isotopes due to the high cost of the isotope analyses.

3.2.1. Aqueous geochemistry of the various microcosms

The density and porosity of the pooled sediment slurries (n = 18, three replicates per microcosm) used for the batch systems were 1.17 ± 0.03 g/cm^3 and 0.84 ± 0.03 g/cm^3, respectively, and the moisture and organic content were 71.0 ± 2.0% and 8.4 ± 0.6%, respectively.

In all of the biotic systems (n = 5), the pH slightly increased from 6.9 ± 0.03 to 7.0 ± 0.02 over the first 24 h and remained constant thereafter, whereas the redox potential slightly declined over time (i.e. −199 ± 7 mV to −254 ± 4 mV), indicating that more reducing conditions had developed (Fig. 2a, b). In contrast, the abiotic microcosms (A1) exhibited different values when compared to the biotic microcosms. In the abiotic microcosms, the initial Eh was 40 mV, which indicated slightly oxic conditions in the sediments as a result of sterilization (autoclaving), but the redox potential decreased to −218 mV after the 96 h incubation period. The pH remained fairly stable (from 6.9 to 6.7) over the 96 h incubation period.

Sulfide concentrations (Fig. 2c) slightly increased throughout the experiment in the N1 (from 0.30 to 0.45 µM) and T1 (from 0.29 to 0.71 µM) microcosms after an initial decrease over 24 h. The SRB-inhibited microcosms (T2 and T4) behaved differently with higher initial sulfide concentrations of 9.53 µM (T2) and 8.97 µM (T4) and showed a slight decrease over time to 8.35 and 7.11 µM, respectively, which is consistent with the low SRR (T3: 0.1 nmol/cm/d, and T4: 0.9 nmol/cm/d). This indicates that there was a near complete inhibition (99–100%) of the sulphate-reducing activity by sodium molybdate. In the abiotic system (A1), the sulfide concentration slightly increased over 46 h from 0.65 to 0.74 µM, which was inconsistent with the complete inhibition of SRB activity (SRR = 0.1 nmol/cm/d). It is likely that the production of sulphide species in the abiotic microcosm was caused by the dissolution of pre-existing iron sulfide minerals, as suggested by

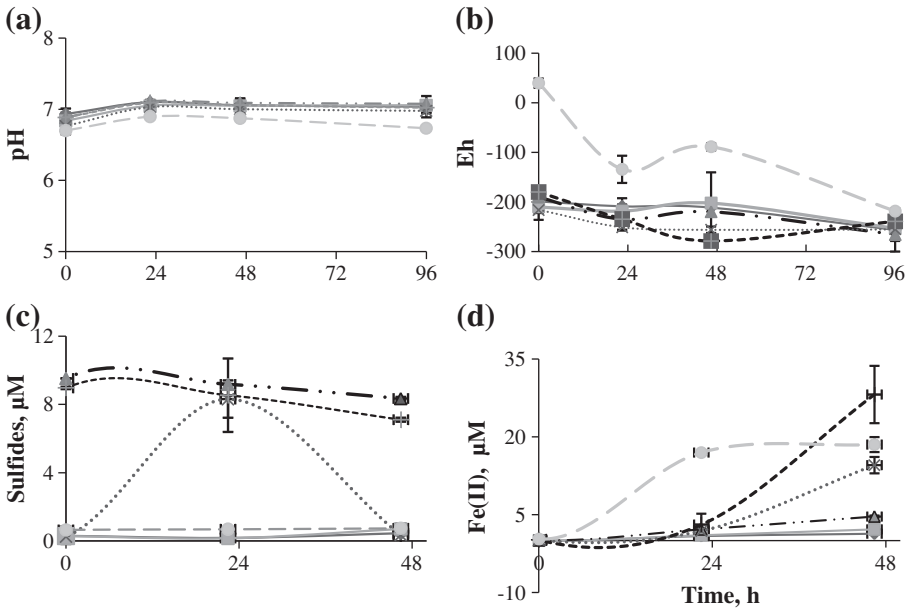

Fig. 2. Porewater characteristics during the 46/96 h microcosm incubations: N (♦),T1 (■), T2 (▲), T3 (×), T4 (+), A1 (●) (pH (a), and Eh (b), sulfides (c), ferrous iron (d)). Error bars represent standard error (SE). The description of the microcosms is presented in Table 1.

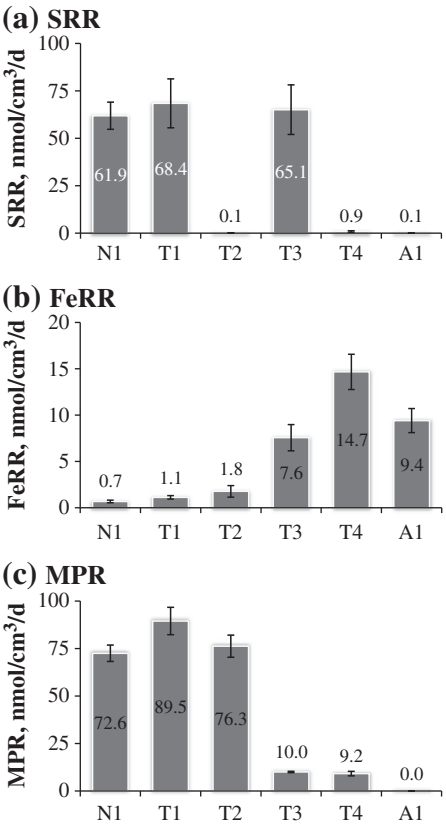

Fig. 3. Sulfate reduction rates (a), iron reduction rates (b), and methane production rates (c) in the St. Lawrence River incubation microcosms. Error bars represent the standard error (SE) for n = 3 replicates. The microcosms' description is in Table 1.

saturation index calculations (Phreeqci-2.15.0). The relatively high SRR (61.9 ± 7.2 nmol/cm/d) of the natural N1 microcosm indicates the existence of an active SRB population in the Zone 1 of the St. Lawrence River sediments. The SRR increased slightly in the T1 (68.4 ± 12.9 nmol/cm/d) and T3 (65.2 ± 13.1 nmol/cm/d) microcosms, when compared to the natural system (N1: 61.9 ± 12.4 nmol/cm/d). The small increase in SRR in the T3 microcosm proved that the BES inhibitor of MPA activity did not affect the activity of SRB (Fig. 3). The differences among the SRR values of the N1, T1 and T3 microcosms, as well as those among the T2, T4 and A1 microcosms were not statistically significant ($p>0.05$), whereas in between those two groups, the differences were statistically significant due to the complete inhibition of SRB activity in the molybdate inhibited (99–100%) and abiotic microcosms (100%).

Ferrous iron (Fe(II)) concentrations increased constantly throughout the experiment in all microcosms (Fig. 2d), with the lowest increase observed in the N1 and T1 microcosms (from 0.01 to 1.32 and 2.17 μM, respectively). The highest increase occurred in the T4 microcosm (from 0.14 to 28.15 μM), followed by the abiotic (A1: from 0.32 to 18.50 μM) and T3 (from 0.09 to 14.53 μM) microcosms. The iron reduction rates (FeRR) were calculated from the linear increase of Fe(II) over 46 h for all treatments (Fig. 3b). The FeRR of the natural (N1) microcosm was low (0.7 ± 0.1 nmol/cm/d), indicating that iron reducers were possibly active in the sediments of Zone 1 of the St. Lawrence River. A slight FeRR increase of 1.7 and 2.6 times, respectively, was observed for the T1 (1.1 ± 0.2 nmol/cm/d) and T2 (1.8 ± 0.6 nmol/cm/d) microcosms, but the differences were not statistically significant ($p<0.05$). The highest rate (14.7 ± 1.9 nmol/cm/d) was determined in the T4 microcosm where both SRB and MPA were inhibited, followed by T3 (7.6 ± 1.4 nmol/cm/d) and A1 (9.4 ± 1.3 nmol/cm/d). No statistically significant differences were observed between the FeRR of the T3, T4 and A1 microcosms, but the differences were statistically significant ($p<0.05$) between the FeRR of those microcosms (T3, T4, and A1) and the others. Saturation index calculations (Phreeqci 2.15.0) showed that the N1, A1, and T1 systems were undersaturated with respect to FeS and mackinawite throughout the course of the experiment, indicating that the iron reduction rates were not biased by the precipitation of iron sulfides in those treatments. In contrast, the microcosms treated with microbial inhibitors (T2, T3, and T4) were all saturated with respect to mackinawite after 24 h of incubation (although all, but T2, became undersaturated again after 46 h), suggesting that the FeRR might be underestimated for those microcosms (Fig. 3b). In addition, the calculations indicated that the microcosms were saturated with respect to more stable iron sulfides, such as pyrite. However, their formation cannot be ascertained here because no mineralogical analyses were performed.

The relatively high methane production rates (MPR) (N1: 72.6 ± 4.3 nmol/cm/d) indicated the existence of an active MPA population in the Zone 1 St. Lawrence River sediments (Fig. 3). The methanogenic activity of the T1 (89.5 ± 7.2 nmol/cm/d) and T2 microcosms (76.3 ± 5.8 nmol/cm/d) (with active SRB and FeRP) increased (in comparison to the N1 microcosm), but the difference was not statistically significant ($p>0.05$). In the two systems (T3 and T4) treated with BES, the methanogenic activity was reduced by 90% (10 ± 0.3 nmol/cm/d and 9.2 ± 1.2 nmol/cm/d, respectively), whereas methane production was 100% inhibited in the abiotic microcosm (0.04 nmol/cm/d). The MPR differences between the inhibited (T3 and T4) and abiotic (A1) microcosms were statistically significant, as well as those between the same inhibited and abiotic microcosms and the other microcosms ($p<0.05$).

Zone 1 of the St. Lawrence River near Cornwall (Zone 1 SLR) is known to be an ebullition site releasing many gases (i.e. CO_2, CO, H_2, and methane) from the sediments to the water column and atmosphere (Poissant et al., 2007; Razavi, 2008). Measurements performed at the St. Lawrence River near Cornwall by Poissant et al. (2007) showed that the fluxes of gases released from the sediments were a mixture of CO_2, CO, H_2 and methane varying between 10^{-6} mg/m^2/h (H_2) and 3.5 mg/m^2/h (CH_4). Moreover, recent work of Razavi (2008) showed that the Zone 1 SLR bubbling rates ranged from less than 1 to cca 2800 mL/m^2/d (<5 to ~169 mg/m^2/h) and that the methane content in the gas ranged from 29 to 84% over their sampling season. Those values translate into a range of methane production rates of <31 to 1054 nmol/cm/d (assuming that 1 g ww = 1 ml = 1 cm^3), which is comparable to the MPR range determined in the different microcosms (i.e., N1: 72.6 nmol/cm/d).

In summary, all systems developed anoxic conditions during the course of the experiment, which represented suitable conditions for either microbial iron or sulfate reduction, as well as for methanogenesis, as indicated by the measured iron, sulfate reduction, and methane production rates. In addition, SRR values reported here are similar to those measured in aquatic environments, such as lake sediments (50–600 nmol/cm/d, (Ingvorsen et al., 1981; Meier et al., 2000; Gough et al., 2008)). Regarding the calculated FeRR for the various microcosms, the values are in agreement with those reported for lake sediments (<0.1 μmol/g/d, (Blodau et al., 2002); 9.6–69.3 μmol/g/d, (Wendt-Potthoff et al., 2002)).

3.2.2. Hg species transformation

The amounts of methylated mercury derived from the inorganic ^{200}Hg spike and demethylated mercury derived from the MM^{199}Hg spike were calculated as in Hintelmann et al. (2000, 2003). A slight linear increase over 96 h was observed for ambient MMHg concentrations (Fig. 4a) in all microcosms, with T3 ($r^2 = 0.97$) having the highest increase, followed by T1 ($r^2 = 0.88$) and N1 ($r^2 = 0.68$). No increases were observed in the T2, T4 and A1 microcosms ($r^2 = 0.54$, 0.48, and 0.35, respectively). In contrast, the MMHg produced from the inorganic mercury spike (^{200}Hg) had a linear increase for the first 46 h in all treatments, after which a slow-down was achieved in all microcosms (Fig. 4b). The observed change in MMHg production from

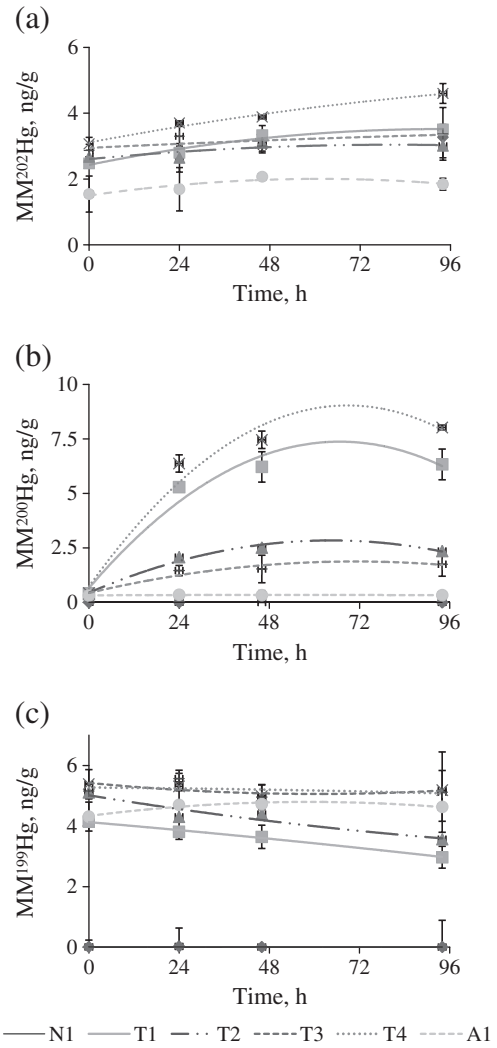

Fig. 4. Ambient MMHg trend (a) along with the evolution of MMHg produced (ng/g d. w., n = 2) from the isotope-enriched mercury spikes ^{200}Hg (b) and Me^{199}Hg (c) during the 96 h microcosm incubations (July 2007): N (♦), T1 (■), T2 (▲), T3 (×), T4 (+), A1 (●).The microcosms' description is in Table 1.

the added inorganic Hg spike (after 46 h) was possible either because demethylation may have slowed down the net increase in MMHg once sufficient MMHg was produced, or gross methylation may have stopped (MM^{200}Hg production). The T3 and T1 microcosms showed the highest methylmercury increase (ng/g) from the inorganic Hg tracer, with T1 also having the highest methylmercury decrease of the added MMHg spike (MM^{199}Hg), which might explain why the change was reached after 46 h in the T1 system. In contrast, the T3 microcosm had the lowest decrease MMHg (199 isotope) among the Hg spiked microcosms (Fig. 4c). The added MMHg spike linearly decreased for 96 h in the T1 and T2 microcosms, but almost no change was observed for the MPA-inhibited (T3 and T4) and abiotic (A1) microcosms. In general, for all microcosms, the demethylation of added MMHg took place very quickly with a constant decrease over the 96-hour incubation period. A similar trend (i.e., higher methylation for T3 and T1 and no/low methylation with SRB inhibited T2 and T4) was observed for the added inorganic spike and the ambient Hg during the incubation, which suggests that methylation of ambient and spiked mercury followed the same pathway. However, the different orders of magnitude might be due to the different availability of the two Hg sources. A small increase of ambient MMHg was observed in the natural microcosm (N1) which may suggest that the addition of the spikes also increased the availability of ambient Hg for methylation in the spiked microcosms (Hintelmann et al., 2000; Drott et al., 2008a,b). However, we cannot exclude the fact that the experimental conditions and manipulations (i.e. temperature change, slurry formation) might have disrupted the natural conditions, establishing a new steady state concentration of MMHg.

The total percentages of mercury methylated and methylmercury demethylated (46 and 96 h incubations) are presented in Table 3. The highest Hg methylation percentage was observed in the microcosms where MPA was inhibited (T3), followed closely by the T1 microcosm (Table 3). This trend was observed not only for methylation of the added inorganic Hg tracer (i.e. 11% T3 and 9.5% T1), but also for the ambient MMHg (i.e. 0.5% T3 and 0.4% T1), supporting once again the fact that the ambient and the added mercury followed the same pathway despite potential availability differences between the tracer and the ambient Hg. Regarding the MMHg demethylation potential, a larger fraction of the added MMHg was demethylated in the T1 microcosm (40.41%; MPR = 89.5 nmol/cm/d) compared to T3 (6.75%), which is in agreement with the approximately 90% MPA inhibition (MPR = 10 nmol/cm/d) in the T3 microcosms.

With respect to the microcosms (T2 and T4) containing the SRB inhibitor, both systems had comparable methylating potentials (2.56% and 2.14%, respectively), but very different demethylating potentials (96 h), with the largest MMHg fraction demethylated in T2 (44.40%) while the T4 microcosm showed the lowest demethylation potential among all microcosms (1.55%). These results corresponded with the microbial activity found in each microcosm. Methanogens activity was enhanced in the T2 microcosms (MPR = 76.3 nmol/cm/d) when SRB were inhibited, but it slowed down (90%) in the T4 microcosms (MPR = 9.2 nmol/cm/d) when the BES inhibitor was applied along with molybdate. Moreover, the addition of BES stimulated not only the methylation of the added inorganic Hg isotope tracer but also the methylation of the ambient Hg in the T3 microcosm (0.51%). In contrast, the addition of sodium molybdate inhibited the methylation of both the added inorganic tracer and ambient mercury in the T2 (i.e. 0.28% for ambient Hg) and T4 (i.e. 0.28% for ambient Hg) microcosms (Table 3 and Fig. 4). The decrease of the demethylation capacity by inhibition of MPA supports the importance of methanogens in MMHg demethylation in aquatic sediments, but the involvement of SRB in demethylation cannot be ruled out since the T4 microcosm had the lowest demethylation potential aside from the abiotic microcosms (A1). Methanogens, as well as SRB, can use C1 organic compounds (i.e. MMHg) as carbon sources and they are known to be involved in oxidative demethylation (OD) in anoxic sediments (Oremland et al., 1995; Marvin-Diapasquale and Oremland, 1998; Marvin-Diapasquale et al., 2000). The methylation potentials for the added inorganic tracer and the ambient Hg were significantly lower in the abiotic (A1) microcosms (Table 4), showing that abiotic processes might have a limited contribution to net MMHg production in those systems. In conclusion, the percentage of MMHg newly generated from the added inorganic Hg spike and the fraction of MeHg demethylated varied with the type of microbes inhibited and our values are in agreement with those reported by Hintelmann et al. (2000).

Table 4
Comparison of potential mercury methylation (M) and methylmercury demethylation rates (D) calculated from the tracer experiment with the St. Lawrence River sediments (calculated for t = 46 h).

Microcosm	$M_{ambient\ Hg}$ pmol/g/h	$M_{Hg(II)spike}$ pmol/g/h	$D_{MMHg\ spike}$ pmol/g/h	([ΣMMHg]/[THg])$_{t=0\ h}$	([ΣMMHg]/[THg])$_{t=46\ h}$
N1	0.08	n/a	n/a	0.2%	0.3%
T1	0.09	0.59	0.05	0.4%	0.7%
T2	0.04	0.22	0.07	0.8%	1.0%
T3	0.08	0.72	0.04	0.4%	0.8%
T4	0.01	0.12	0.02	0.4%	0.5%
A1	0.05	0	−0.04	0.6%	0.6%

The potential mercury methylation and methylmercury demethylation rates (pmol/g/h) calculated for the 46 h incubation period for the added isotope-enriched tracers ($^{200}Hg^{2+}$ and $Me^{199}Hg^{+}$) are presented in Table 4. The process of $^{200}Hg^{2+}$ methylation varied with the type of microbes inhibited, and the highest calculated rate (among inhibited assays) was in the microcosms where methanogenesis was inhibited (T3: 0.72 pmol/g/h) and the lowest rates were found in the microcosms where both SRB and MPA were inhibited (T4: 0.12 pmol/g/h). No methylation of the added inorganic Hg tracer was observed in the abiotic (A1) microcosms (Table 5). The SRB-inhibited microcosms (T2 and T4) had potential methylation rates four times lower than the other ones. In contrast, the demethylation rate determined for the added methylmercury spike was the highest for the T2-SRB-inhibited microcosm followed by the T1 microcosm (Table 4). The MPA-inhibited microcosms had the lowest demethylation rates among all microcosms, which is in agreement with the methylation rates. Moreover, the addition of inhibitors influenced not only the methylation and demethylation of the tracers in the four microcosms, but also the evolution of ambient MMHg. The rates were doubled in the T1 and T3 assays in comparison with the SRB-inhibited (T2 and T4) and abiotic (A1) microcosms.

The potential methylation rates determined in this study suggest that the activity of MPA is important for the demethylation process. For the methylation process, other processes, such as FeRP activity, should be considered beside SRB activity. The inhibition of both SRB and MPA (T4) enhanced the activity of iron-reducing prokaryotes (FeRP), as demonstrated by the increase of FeRR in the inhibited microcosms (Fig. 3b). It is known that iron can affect mercury methylation by either altering the availability of Hg (Warner et al., 2003; Mehrotra and Sedlak, 2005; Feyte et al., 2010) or enhancing the activity of FeRP with respect to other microorganisms, in particular SRB (Flemming et al., 2006; Kerin et al., 2006; Warner et al., 2003). Moreover, Oremland et al. (1995) detected substantial oxidative demethylation at a site where sulfate reduction and methanogenesis rates were low, and suggested that other respiratory anaerobes (e.g., denitrifiers and Fe(III) and Mn(IV) reducers) may also carry out oxidative demethylation, which represents an explanation for the lower but detectable demethylation rate measured in the T4 (SRB and MPA inhibited) microcosm when compared to the T2 microcosm.

3.2.3. Potential methylation and demethylation rate constants

In order to verify whether the methylation or demethylation rates were dependent on the amount of tracers added, as previously suggested by Hintelmann et al. (1995, 2000), we calculated the rate constants (K_m and K_d), which by definition are independent of the amount spiked. The potential rate constants calculated from the evolution of isotope-enriched MMHg trends over 46 h (96 h for K_d) are presented in Table 5 along with data from other studies.

Potential methylation rate constants (K_m) differed significantly among microcosms. The MPA-inhibited microcosm (T3) had the highest rate constant (0.016 d^{-1}), followed by the T1 microcosm (0.015 d^{-1}). The SRB-inhibited microcosms had comparable potential methylation rate constants (T2: 0.003 d^{-1} and T4: 0.002 d^{-1}) while the abiotic (A1) microcosm K_m was almost zero (0.0001 d^{-1}). The trends observed for K_m values in all microcosms are in agreement with the calculated potential methylation rates (M) (Table 4). For the demethylation, the K_d values were calculated for the whole period (96 h) in order to increase the statistical power. The highest value (1.7 d^{-1}) was in the T2-SRB-inhibited microcosm followed by the T1 microcosm (1.4 d^{-1}). Both MPA-inhibited microcosms (T3 and T4) had similar low K_d rates (0.3 d^{-1} and 0.2 d^{-1}), which is in agreement with the high degree of inhibition of methanogenesis (90% with respect to T1). The K_d values are in agreement with the K_m values and also with the methylation potential (M) and demethylation rates (D) (Table 4).

Our results indicate the importance of SRB in Hg methylation in freshwater systems, as reported in other studies (i.e. Compeau and Bartha, 1985; Oremland et al., 1995; King et al., 2000, 2001, 2002; Flemming et al., 2006). For instance, Matilainen (1995) observed that molybdate addition inhibited methylation in sediments from four

Table 5
Comparison of specific mercury methylation and methylmercury demethylation rate constants calculated from various tracer studies.

Site/sediment	Rate constant[a]			MMHg[b]		Reference
	Km	Kd	Half-life	Predicted	Measured	
	(d^{-1})	(d^{-1})	(d)	(ng/g)	(ng/g)	
N1–SLR 2007	n/a	n/a	n/a	2.1	2.9	This study
T1–SLR 2007	0.02	1.4	0.5	2.6	2.8	This study
T2–SLR 2007	0	1.7	0.4	2.5	2.6	This study
T3–SLR 2007	0.02	0.3	2.6	3.3	3.7	This study
T4–SLR 2007	0	0.2	3	3	3.3	This study
A1–SLR 2007	0	0.03	25.5	1	1.7	This study
N–Mer Bleue, On	n/a	n/a	1.6	0.6	0.6	Avramescu (2010)
T1–Mer Bleue, On	0.05	0.28	2.4	1.4	1.6	Avramescu (2010)
T2–Mer Bleue, On	0.03	0.06	10.9	0.5	0.5	Avramescu (2010)
T3–Mer Bleue, On	0.06	0.22	3.2	0.8	0.9	Avramescu (2010)
T4–Mer Bleue, On	0.02	0.12	5.8	0.5	0.4	Avramescu (2010)
Ranger Lake, On	0.01	0.42	1.7	2.8	1.8	Hintelmann et al. (2000)
Lake Vernon, On	0.02	0.53	1.3	3	0.8	Hintelmann et al. (2000)
Lake Vernon, On	0.01	0.48	1.5	2.5	0.8	Hintelmann et al. (1995)
Brakish water estuary (Köp)	0	0.07				Drott et al. (2008a)
Brakish water estuary (Sku)	0	0.54				Drott et al. (2008a,b)
Low productive freshwater (Kar)	0	0.05				Drott et al. (2008a,b)
Low productive lake (Ala)	0	0.02				Drott et al. (2008a,b)
High productive freshwaters	0.02	0.12				Drott et al. (2008a,b)
Adour River Estuary, France (biotic)	0.03	0.07				Martin-Doimeadios et al. (2004)
Adour River Estuary, France (abiotic)	0	0.24				Martin-Doimeadios et al. (2004)
Hudson River, New York (whole core)	0	15.84				Heyes et al. (2006)
Bay of Fundy, Canada (whole core)	0.03	5.76				Heyes et al. (2006)
Bay of Funday (zone of greatest methylation potential)	0.04	3.60				Heyes et al. (2006)
Patuxent River (whole core)	0.01					Heyes et al. (2006)
Gironde Estuary, France	0	2.64				Schäfer et al. (2010)

[a] Rate constants are for inorganic Hg (K_m) and MMHg (K_d, half-life) spike, respectively.
[b] Comparison is for ambient MMHg.

lakes in Finland, and suggested that acetate-utilizing SRB were the main methylators under sulfate limiting conditions. In addition, in anoxic estuarine sediments, inhibition of methanogenesis stimulated the SRB activity and Hg methylation, when sulfate was limiting (Compeau and Bartha, 1985). Finally, Lovley and Klug (1983) showed that SRB were able to outcompete methanogens, even in sulfate limited freshwater sediments.

The rate constants K_m and K_d for ambient Hg were obtained by fitting the experimental data ($MM^{202}Hg$), according to Hintelmann et al. (2000). The XLfit software was used to fit the curve and the results are presented in Table S1 (Supporting information). The ambient MMHg concentrations in the microcosms were predicted by applying the calculated ambient rate constants (Table 5). In other tracer studies (Hintelmann et al., 2000), discrepancies that were observed between the predicted and measured ambient MMHg concentrations were considered as an indication that the inorganic Hg tracer was more bioavailable than the ambient mercury. As shown in Table 5 (details in Table S1), a relatively good agreement was obtained between the predicted and measured values of ambient methylmercury. In contrast, if we consider the fraction of Hg present as MMHg, the values were slightly higher for the tracer isotope (199 isotope: 0.24–0.50%) when compared to the ambient Hg (202 isotope: 0.09–0.25%) (Table S2, Supporting information), and this supports the fact that the tracers were more available than the ambient Hg.

The demethylation rate constants translated into a relatively long half-life ($t_{½}$) of the ambient MMHg in sediments (i.e., 8.3 d^{-1}), higher than those measured for a pristine wetland (Avramescu, 2010) or observed in other studies (Hintelmann et al., 2000; (1.8 d^{-1})).The half-life of the added tracers varied from 0.4 and 0.5 d^{-1} in the T2 (SRB inhibited) and T1 microcosms, respectively, and from 2.6 and 3.0 d^{-1} in the MPA-inhibited microcosms (T3 and T4, respectively). In the abiotic microcosm, the half-life was 25.5 d^{-1}, which indicates that the abiotic process contributed less to the net demethylation. As indicated by the half-life values, the added MMHg-tracer (0.5 d^{-1} in T1) was more available for demethylation than the ambient one (8.3 d^{-1} in T1, as in Table S1). We also observed that for the St. Lawrence River system, the inhibition of MPA increased the residence time of MMHg in the sediments, which in turn can lead to an increased exposure of biota to MMHg. In contrast, the inhibition of SRB decreased the residence time of MMHg in the sediments. Considering the decrease in demethylation rate constants in MPA-inhibited microcosms (T3 and T4) when compared to T1 (Table 5), we can conclude that oxidative demethylation by methanogens may be an important pathway for MMHg demethylation in the SLR sediments. Given the long history of contamination of the investigated SLR sediments (Delongchamp et al., 2009), we cannot ignore the importance of reductive demethylation (RD) by *mer* operon. The *mer* detoxification is extensive in aquatic environments, being induced at lower Hg^{2+} and oxygen concentrations (aerobic and facultative mercury resistant microbes). MMHg can be degraded reductively by *mer* operon functions to CH_4 and elemental Hg^0, in contrast to oxidative demethylation, which degrades MMHg to CO_2, along with a small amount of CH_4 and ionic Hg^{2+}(Barkay et al., 2003). In anaerobic sediment settings, the prevalence of either RD or OD is important, influencing the MMHg production especially in Hg-contaminated sediments since the *mer* operon process results in a net removal of Hg from the sediments (as Hg^0), whereas OD producesHg^{2+} and may fuel the methylation process within the sediments (Barkay et al., 2003). Whether the *mer*-mediated demethylation takes place at the same time as OD in SLR sediments has yet to be determined.

3.2.4. Relationship between the rate constants, SRR, FeRR, MPR, % MMHg and porewater geochemistry

We evaluated the relationship between the rate constants (K_m and K_d) calculated under laboratory conditions with sulfate reduction rates, methane production rates and iron reduction rates, as well as some porewater characteristics. Our results indicate that K_m ($r^2 = 0.98$, $p<0.05$), but not K_d ($r^2 = 0.08$), is positively correlated with SRR (i.e., the higher the SRR, the higher the Km values) (Fig. 5a), which strongly suggests that SRB are involved in Hg methylation, but may not be implicated in MMHg demethylation in the SLR sediments. An inverse relationship was observed with MPR, with K_d ($r^2 = 0.61$) being positively correlated with MPR but not K_m ($r^2 = 0.10$), showing that in contrast to SRB, methanogens are involved in MMHg demethylation in the Zone 1 SLR sediments (Fig. 5b). In addition, FeRR were negatively correlated with K_m ($r^2 = 0.19$) and K_d ($r^2 = 0.81$) (Fig. 5c). The increase in FeRR therefore corresponds to a decrease in demethylation, which suggests that iron reduction may influence net methylation in the Zone 1 SLR sediments by decreasing demethylation rather than favouring methylation in the long term. This is supported by the negative relationship obtained between the porewater Fe(II) and MMHg spike concentrations ($r^2 = 0.26$–0.88) in the T1 and T3 microcosms; however these relationships are only significant ($p<0.05$, $df = 4$) for the T1 microcosm.

4. Conclusions

Our results first indicate that Hg spike addition increased the availability of ambient Hg for methylation in all treatments, with the exception of the SRB-inhibited microcosms (T2). The inhibition of certain groups of microbes clearly had an effect on methylation and demethylation. For instance, the highest calculated methylation percentage was in the microcosm where only methanogens were

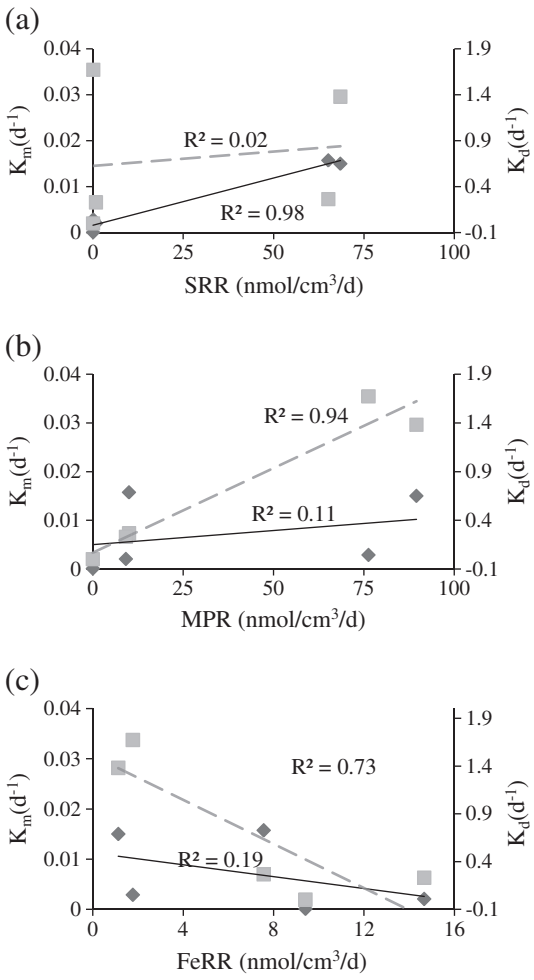

Fig. 5. Relationship between K_m (♦) or K_d (■) and percent MMHg to THg (a), sulfate reduction rates (b), methane production rates (c), and iron reduction rates (c) for all microcosm. K_m and K_d calculated for 46 h as in Table 5.

inhibited (T3), followed closely by the Hg spike control system (T1). Given the fact that the methylation potential was greatly decreased in the abiotic and SRB-inhibited microcosms, we can conclude that methanogens play an important role in Hg methylation because they limit methylation. Moreover, their inhibition in the microcosms favored the growth of sulfate reducers and/or iron reducers. To clarify the role of FeRP in net Hg methylation, further experiments should be carried out with hydrous ferric oxide amendments to the sediments, along with isotopic Hg additions and microbial inhibitors.

In addition, it is generally accepted that methanogens, as well as SRB, are involved in oxidative demethylation in anoxic sediments, and our data indicate that in the St. Lawrence river sediments from Zone 1, methanogens might have had the leading role in MMHg demethylation. Results from our study also show that abiotic demethylation pathways have the lowest contribution to net MMHg production in the sediments.

Acknowledgements

L. Avramescu was supported by a NSERC graduate scholarship. The research was carried out with an NSERC Discovery grant to D. Lean, and a Best in Science Grant to J. Ridal from the Ontario Ministry of the Environment, Canada. The authors acknowledge the St. Lawrence River Institute of Environmental Sciences in Cornwall for technical and sampling support. The authors are also grateful to Vanessa Mongeon, Jonathan Mayo and Willy de Wit for their assistance during sampling and to Joy Zhu, for helping with isotope analysis.

Appendix A. Supplementary data

Supplementary data to this article can be found online at doi:10.1016/j.scitotenv.2010.11.016.

References

Avramescu M-L. Biogeochemical Factors Influencing Net Mercury Methylation in Contaminated Freshwater Sediments from the St. Lawrence River in Cornwall, Ontario, Canada. Ph.D. Thesis, University of Ottawa, Ottawa, ON, Canada, 2010; 116 page.

Avramescu M-L, Zhu J, Yumvihoze E, Hintelmann H, Fortin D, Lean DRS. A simplified sample preparation procedure for measuring isotope enriched methylmercury. Environ Toxicol Chem 2010;29:1256–62.

Balch WE, Wolfe RS. Specific and biological distribution of coenzyme M (2-mercaptoethane sulfonic acid). J Bacteriol 1979;137:264–73.

Baldi F, Parati F, Filipelli M. Dimethylmercury and dimethylmercury-sulfide of microbial origin in the biogeochemical cycle of Hg. Water Air Soil Pollut 1995;80:805–15.

Barkay T, Miller SM, Summers AO. Bacterial mercury resistance from atoms to ecosystems. FEMS Microbiol Rev 2003;27:355–84.

Benoit JM, Gilmour CC, Heyes A, Mason RP, Miller CL. Geochemical and biological controls over methylmercury production and degradation in aquatic ecosystems. ACS Symp Ser 2003;835:262–97.

Blodau C, Roehm CL, Moore TR. Iron, sulfur and dissolved carbon dynamics in a northern peatland. Arch Hydrobiol 2002;154:561–83.

Biberhofer J, Rukavina NA. Data on the distribution and stability of St. Lawrence River sediments at Cornwall, ON. National Water Research Institute, Environment Canada; 2002. Contribution Number 02-195.

Canadian Council of Ministers of the Environment (CCME). Protocol for the derivation of Canadian sediment quality guidelines for the protection of aquatic life: summary tables—Update 2002. CCME EPC-98E; 2005; Prepared by Environment Canada, Guidelines Division, Technical Secretariat of the CCME Task Group on Water Quality Guidelines, Ottawa; 2002.

Canario J, Poissant L, O'Driscoll N, Vale C, Pilote M, Lean D. Sediment processes and mercury transport in a frozen freshwater fluvial lake (Lake St. Louis, QC, Canada). Environ Pollut 2009;157:1294–300.

Celo V, Scott S, Lean DRS. Abiotic pathways of mercury methylation in the aquatic environment. Sci Total Environ 2006;368(1):126–37.

Chen Y, Bonzongo JC, Miller GC. Inhibition of mercury methylation in anoxic freshwater sediment by group VI anions. ACS Division Environ Chem 1996;36:55–7 Preprints.

Clarkson TW. Human toxicology of mercury. J Trace Elem Exp Med 1998;11:303–17.

Cline JD. Spectrophotometric determination of hydrogen sulfide in natural waters. Limnol Oceanogr 1969;14:454–8.

Compeau G, Bartha R. Sulfate-reducing bacteria: principal methylators of mercury in anoxic estuarine sediments. Appl Environ Microbiol 1985;50:498–502.

Delongchamp TM, Lean DRS, Ridal JJ, Blais JM. Sediment mercury dynamics and historical trends of mercury deposition in the St. Lawrence River area of concern near Cornwall, Ontario, Canada. Sci Total Environ 2009;407:4095–104.

Delongchamp TA, Ridal JJ, Lean DRS, Poissant L, Blais JM. Mercury transport between sediments and the overlying water of the St. Lawrence River area of concern near Cornwall, Ontario. Environ Pollut 2010;158:1487–93.

Drott A, Lambertsson L, Björn E, Skyllberg U. Do potential methylation rates reflect accumulated methyl mercury in contaminated sediments? Environ Sci Technol 2008a;42:153–8.

Drott A, Lambertsson L, Björn E, Skyllberg U. Potential demethylation rate determinations in relation to concentrations of MeHg, Hg and porewater speciation of MeHg in contaminated sediments. Mar Chem 2008b;112:93-101.

Eckley CS, Hintelmann H. Determination of mercury methylation potentials in the water column of lakes across Canada. Sci Total Environ 2006;368(1):111–25.

Eckley CS, Watras CJ, Hintelmann H, Morrison K, Kent AD, Regnell O. Mercury methylation in the hypolimnetic waters of lakes with and without connection to wetlands in northern Wisconsin. Can J Fish Aquat Sci 2005;62:400–11.

Falter R. Experimental study on the unintentional abiotic formation of inorganic mercury during analysis: Part 1: localisation of the compounds effecting the abiotic mercury methylation. Chemosphere 1999;39:1051–73.

Feyte S., Tessier A., Gobeil C., Cossa, D. In situ adsorption of mercury, methylmercury and other elements by iron oxyhydroxides and organic matter in lake sediments. Appl Geochem 2010;25(7):984–995.

Flemming EJ, Marck EE, Green PG, Nelson DC. Mercury methylation from unexpected sources: molybdate-inhibited freshwater sediments and an iron-reducing bacterium. Appl Environ Microbiol 2006;72:457–64.

Gilmour CC, Henry EA. Mercury methylation in aquatic systems affected by acid deposition. Environ Pollut 1991;71:131–69.

Gough HL, Dahl AL, Tribou E, Noble PA, Gaillard J-F, Stahl DA. Elevated sulfate reduction in metal-contaminated freshwater lake sediments. J Geophys Res G: Biogeosci 2008;113(4) art. no. G04037.

Hammerschmidt CR, Fitzgerald WF, Lamborg CH, Balcom PH, Visscher PT. Biogeochemistry of methylmercury in sediments of Long Island Sound. Mar Chem 2004;90:31–52.

Heyes A, Mason R, Kim E-H, Sunderland E. Mercury methylation in estuaries: insights from using measuring rates using stable mercury isotopes. Mar Chem 2006;102:134–47.

Hintelmann H, Evans RD, Villeneuve JY. Measurement of mercury methylation in sediments by using enriched stable mercury isotopes combined with methylmercury determination by gas chromatography-inductively coupled plasma mass spectrometry. J Anal At Spectrom 1995;10:619–24.

Hintelmann H, Evans RD. Application of stable isotopes in environmental tracer studies—measurement of monomethylmercury (CH_3Hg^+) by isotope dilution ICP-MS and detection of species transformation. Fresenius J Anal Chem 1997;358:378–85.

Hintelmann H, Keppel-Jones K, Evans RD. Constants of mercury methylation and demethylation rates in sediments and comparison of tracer and ambient mercury availability. Environ Toxicol Chem 2000;19:2204–11.

Hintelmann H, Ogrinc N. Determination of stable mercury isotopes by ICP/MS and their application in environmental studies. In: Cai Y, Braids CO, editors. Biogeochemistry of environmentally important trace elements, 835. ACS Symp. Series; 2003. p. 321–38.

Ingvorsen K, Zeikus JG, Brock TD. Dynamics of bacterial sulfate reduction in a eutrophic lake. Appl Environ Microbiol 1981;42:1029–36.

Jørgensen BB. A comparison of methods for the quantification of bacterial sulfate reduction in coastal marine sediments. I. Measurement with radiotracer techniques. Geomicrobiol J 1978;1:11–27.

Kerin EJ, Gilmour CC, Roden E, Suzuki MT, Coates JD, Mason RP. Mercury methylation by dissimilatory iron-reducing bacteria. Appl Environ Microbiol 2006;72:7919–21.

King JK, Kostka JE, Frischer ME, Saunders FM. Sulfate-reducing bacteria methylate mercury at variable rates in pure culture and in marine sediments. Appl Environ Microbiol 2000;66:2430–7.

King JK, Kostka JE, Frisher ME, Saunders FM, Jahnke RA. A quantitative relationship that demonstrates mercury methylation rates in marine sediments are based on the community composition and activity of sulfate bacteria. Environ Sci Technol 2001;35:2492–6.

King JK, Harmon S, Michele S, Fu TT, Gladden JB. Mercury removal, methylmercury formation, and sulfate-reducing bacteria profiles in wetland mesocosms. Chemosphere 2002;46:859–70.

Koschorreck M. Methane turnover in exposed sediments of an Amazon floodplain lake. Biogeochemisry 2000;50:195–206.

Lovley DR, Klug MJ. Sulfate reducers can outcompete methanogens at freshwater sulfate concentrations. Appl Environ Microbiol 1983;45:187–92.

Martin-Doimeadios R, Tessier E, Amouroux D, Guyoneaud R, Duran R, Caumette P, Donard OFE. Mercury methylation/demethylation and volatilization pathways in estuarine sediment slurries using species-specific enriched stable isotopes. Mar Chem 2004;90:107–23.

Marvin-Diapasquale MC, Oremland RS. Bacterial methylmercury degradation in Florida Everglades peat sediment. Environ Sci Technol 1998;32:2556–63.

Marvin-Diapasquale MC, Agee J, McGowan C, Oremland RS, Thomas M, Krabbenhoft D, Gilmour CC. Methylmercury degradation pathways: a comparison among three mercury- impacted ecosystems. Environ Sci Technol 2000;34:4908–17.

Matilainen T. Involvement of bacteria in methylmercury formation in anaerobic lake waters. Water Air Soil Pollut 1995;80:757–64.

Mehrotra AS, Sedlak DL. Decrease in net mercury methylation rates following iron amendment to anoxic wetland sediment slurries. Environ Sci Technol 2005;39:2564–70.

Merritt KA, Amirbahman A. Mercury methylation dynamics in estuary and coastal marine sediments—a critical review. Earth Sci Rev 2009;96:54–66.

Meier J, Voigt A, Babenzien H-D. A comparison of 35S-SO42-radiotracer techniques to determine sulfate reduction rates in laminated sediments. J Microbiol Meth 2000;41:9-18.
Oremland RS, Miller LG, Dowdle P, Connell T, Barkay R. Methylmercury oxidative degradation potentials in contaminated and pristine sediments of the Carson River, Nevada. Appl Environ Microbiol 1995;61:2745–53.
Oremland RS, Capone DG. Use of specific inhibitors in biogeochemistry and microbial ecology. Adv Microb Ecol 1988;10:285–383.
Otto M. Chemometrics. Statistics and Computer Application in Analytical Chemistry. 2nd Edition. Wiley-VCH Verlag GmbH & Co. KgaA; 2007. p. 183–234.
Pak KR, Bartha R. Mercury methylation and demethylation in anoxic lake sediments and by strictly anaerobic bacteria. Appl Environ Microbiol 1998;64:1013–7.
Poissant L, Constant P, Pilote M, Canário J, O'Driscoll N, Lean DRS. The ebullition of hydrogen, carbon monoxide, methane, carbon dioxide and total gaseous mercury from the Cornwall area of concern. Sci Total Environ 2007;381:256–62.
Praharaj T, Fortin D. Indicators of microbial sulfate reduction in acidic sulfide-rich mine tailings. Geomicrobiol J 2004;21:457–67.
Quemarais B, Cossa D, Rondeau B, Pham TT, Fortin B. Mercury distribution in relation to iron and manganese in the waters of the St. Lawrence River. Sci Total Environ 1998;213:193–201.
Razavi N.R. Role of bubbling from aquatic sediments in mercury transfer to a benthic invertebrate in the St. Lawrence River, Cornwall, Ontario. Master's Thesis, Queen's University, Kingston, ON, Canada, 2008; p. 108.
Richman LA, Dreier SI. Sediment contamination in the St. Lawrence River along the Cornwall, Ontario waterfront. J Great Lakes Res 2001;27:60–83.
Ridal JJ, Yanch LE, Fowlie AR, Razavi NR, Delongchamp TM, Choy ES, et al. Potential causes of enhanced transfer of mercury to St. Lawrence River biota: implications for sediment management strategies at Cornwall, Ontario, Canada. Hydrobiology 2009;647(1):81–98.
Rodier J. L'analyse de l'eau; Eaux naturelles, eaux résiduaires, eau de mer. 8th ed. 1997. Dunod, 1383 pp.
Schäfer J, Castelle S, Blanc G, Dabrin A, Masson M, Lanceleur L, Bossy C. Mercury methylation in the sediments of a macrotidal estuary (Gironde Estuary, south-west France). Estuar Coast Shelf Sci 2010;90:80–92.
Ullrich SM, Tanton TW, Abdrashitova SA. Mercury in the aquatic environment: a review of factors affecting methylation. Crit Rev Environ Sci Technol 2001;31:241–93.
Viollier E, Inglett PW, Hunter K, Roychoudhury AN, Van Cappellen P. The ferrozine method revisited: Fe(II)/Fe(III) determination in natural waters. Appl Geochem 2000;15:785–90.
Warner KA, Roden EE, Bonzongo JC. Microbial mercury transformation in anoxic freshwater sediments under iron-reducing and other electron-accepting conditions. Environ Sci Technol 2003;37:2159–65.
Wendt-Potthoff K, Frommichen R, Herzprung P, Koschorreck M. Microbial Fe(III) reduction in acidic mining lake sediments after addition of an organic substrate and lime. Water Air Soil Pollut Focus 2002;2:81–5.
Wood JM, Kennedy PS, Rosen CG. Synthesis of methylmercury compounds by extracts of a methanogenic bacterium. Nature 1968;220:173–4.
Zar JH. Biostatistical Analysis. 5th edition. New Jersey: Prentice-Hall, Upper saddle River; 2006. p. 208–450.